A Study of the Urban Boundary Layer Using Different Urban Parameterizations and High-Resolution Urban Canopy Parameters with WRF

FRANCISCO SALAMANCA AND ALBERTO MARTILLI

Research Center for Energy, Environment and Technology (CIEMAT), Madrid, Spain

MUKUL TEWARI AND FEI CHEN

National Center for Atmospheric Research, Boulder, Colorado*

(Manuscript received 20 April 2010, in final form 11 November 2010)

ABSTRACT

In the last two decades, mesoscale models (MMs) with urban canopy parameterizations have been widely used to study urban boundary layer processes. Different studies show that such parameterizations are sensitive to the urban canopy parameters (UCPs) that define the urban morphology. At the same time, high-resolution UCP databases are becoming available for several cities. Studies are then needed to determine, for a specific application of an MM, the optimum degree of complexity of the urban canopy parameterizations and the resolution and details necessary in the UCP datasets. In this work, and in an attempt to answer the previous issues, four urban canopy schemes, with different degrees of complexity, have been used with the Weather Research and Forecasting (WRF) model to simulate the planetary boundary layer over the city of Houston, Texas, for two days in August 2000. For the UCP two approaches have been considered: one based on three urban classes derived from the National Land Cover Data of the U.S. Geological Survey and one based on the highly detailed National Urban Database and Access Portal Tool (NUDAPT) dataset with a spatial resolution of 1 km^2. Two-meter air temperature and surface wind speed have been used in the evaluation. The statistical analysis shows a tendency to overestimate the air temperatures by the simple bulk scheme and underestimate the air temperatures by the more detailed urban canopy parameterizations. Similarly, the bulk and single-layer schemes tend to overestimate the wind speed while the multilayer schemes underestimate it. The three-dimensional analysis of the meteorological fields revealed a possible impact (to be verified against measurements) of both the urban schemes and the UCP on cloud prediction. Moreover, the impact of air conditioning systems on the air temperature and their energy consumption has been evaluated with the most developed urban scheme for the two simulated days. During the night, this anthropogenic heat was responsible for an increase in the air temperature of up to 2°C in the densest urban areas, and the estimated energy consumption was of the same magnitude as energy consumption obtained with different methods when the most detailed UCP database was used. On the basis of the results for the present case study, one can conclude that if the purpose of the simulation requires only an estimate of the 2-m temperature a simple bulk scheme is sufficient but if the purpose of the simulation is an evaluation of an urban heat island mitigation strategy or the evaluation of the energy consumption due to air conditioning at city scale, it is necessary to use a complex urban canopy scheme and a detailed UCP.

1. Introduction

Mesoscale models (MMs) in combination with urban canopy parameterizations are increasingly used to investigate the behavior of the urban boundary layer (UBL). The urban parameterizations estimate the mean thermal and dynamic effects of the cities on the atmosphere. The first urban schemes represented the thermal effects of the city using greater heat capacity and thermal conductivity than those used in natural soils to reproduce the large heat storage that takes place in the urban surfaces (Liu et al. 2006). In the same way, large values for roughness parameters were used to represent the momentum sink and the turbulence generated by roughness elements. The disadvantage of these approaches is that they cannot represent the heterogeneities present in the

* The National Center for Atmospheric Research is sponsored by the National Science Foundation.

Corresponding author address: F. Salamanca, Research Centre for Energy, Environment and Technology (CIEMAT), Avenida Complutense 22, 28040 Madrid, Spain.
E-mail: francisco.salamanca@ciemat.es

DOI: 10.1175/2010JAMC2538.1

© 2011 American Meteorological Society

urban areas because of the variability of urban morphology between different neighborhoods. Subsequently, the first single-layer urban canopy models (UCMs) were developed (e.g., Masson 2000; Kusaka et al. 2001; Kanda et al. 2005). They represent the urban geometry by infinitely long street canyons and three different urban surfaces (walls, roofs, and roads), with the exception of Kanda's model that represents the city with a 3D geometry. With these new approaches, several urban classes with different thermal properties and morphology can be considered, and the heterogeneities of the city are better represented. This fact can be important, for example, if we are interested in the spatial distribution of the air temperature within the city. Finally, multilayer urban canopy models (Martilli et al. 2002; Kondo et al. 2005) permitted a direct interaction of the buildings with the planetary boundary layer (PBL). To date, the coupling between simple building energy models and multilayer urban canopy parameterizations (Kikegawa et al. 2003; Salamanca and Martilli 2010) represents the most sophisticated approach and permits the study of the impact of anthropogenic heat (AH) fluxes due to air conditioning on the urban atmosphere. This increasing number of urban parameterizations and the important differences existing between them require a study to show positive and negative points of each approach, to facilitate their use. In this direction, an important effort (Grimmond et al. 2010) has been carried out by comparing energy fluxes obtained with a wide range of urban models run offline, against site observations.

An intensive effort has been carried out for the community mesoscale Weather Research and Forecasting (WRF) model (Chen et al. 2011) to improve its skills in urban areas and to be able to assess environmental problems such as the urban heat island (UHI) and urban air pollution. In this context, in the first part of this article, results obtained with WRF with four different urban canopy parameterizations over the city of Houston, Texas, (see Table 1) are presented. Comparisons against measurements of surface air temperature and wind speed are also shown. The first urban parameterization (included in WRF since 2003) is a bulk scheme (denoted BULK) that represents the effects of urban surfaces by means of a roughness length of 0.8 m, a surface albedo of 0.15 to represent the radiation trapping in the urban canyons, a volumetric heat capacity of 3.0 MJ m^{-3} K^{-1}, and a thermal conductivity of 3.24 W m^{-1} K^{-1} to represent the large heat storage in the urban buildings and roads. This approach has been successfully employed in real-time forecasts (Liu et al. 2006). The second urban parameterization was developed by Kusaka et al. (2001) and Kusaka and Kimura (2004). It is a single-layer urban canopy UCM in which the anthropogenic heat can be added to the sensible heat flux in the urban canopy layer. The urban geometry is represented through infinitely long street canyons, and three different urban surfaces (roof, wall, and roads) are recognized. Shadowing, reflections, and trapping of radiation in the street canyon are considered, and an exponential wind profile is prescribed to deduce the wind speed in the canyon from the wind speed above the canyon, where the lowest grid point of the mesoscale model is located. The sensible heat fluxes from roof, wall, and roads are introduced in the lowest atmospheric layer. This option has been included in WRF (V2.2) since 2006. The third urban parameterization was developed by Martilli et al. (2002), and it is a multilayer urban canopy scheme called BEP (which stands for building effect parameterization; it has included in the WRF V3.1 release since 2009). BEP recognizes the three-dimensional nature of urban surfaces and the fact that buildings vertically distribute sources and sinks of heat and momentum through the whole urban canopy layer. It takes into account the effects of the vertical (walls) and horizontal (streets and roofs) surfaces on momentum, turbulent kinetic energy, and potential temperature. The wall and road radiation consider shadowing, reflection, and trapping of shortwave and longwave radiation in the urban canyons. The last urban parameterization is an extension of the BEP scheme and was developed by Salamanca et al. (2010). It is the result of the coupling between BEP and a simple building energy model (BEM) that improves the results obtained with the old version of BEP (Salamanca and Martilli 2010). BEM accounts for the 1) diffusion of heat through the walls, roofs, and floors; 2) radiation exchanged through windows; 3) longwave radiation exchanged between indoor surfaces; 4) generation of heat due to occupants and equipments; and 5) air conditioning, ventilation, and heating. The BEP+BEM parameterization takes into account the exchanges of energy between the interior of the buildings and the outdoor atmosphere. Consequently, the impact of air conditioning systems (AC) and their energy consumption is estimated. The new BEP+BEM scheme has been included in WRF V3.2 release on April 2010.

In the standard version of WRF, the urban schemes looked up the input parameters for the urban morphology from a table with only three different urban classes (commercial, industrial, and high or low residential areas) that can be derived from land use databases [e.g., the National Land Cover Data for the United States (NLCD), developed by the U.S. Geological Survey (USGS)]. In the simulations with the four urban schemes, the input parameters (building height, urban fraction, building plan area fraction, and building height-to-width ratio) for the three urban classes have been extracted from the reports of Burian and Han (2003) and Burian et al. (2003).

TABLE 1. Overview of the different urban schemes used in the intercomparison.

	BULK	UCM	BEP	BEP+BEM
How the canopy is resolved	No canopy; roughness length modified	Single layer	Multilayer	Multilayer
Anthropogenic heat	No	From fixed temporal profiles	No	From a building energy model
Accounting for fraction of vegetation	No	Yes	Yes	Yes
PBL scheme used in this study	Mellor–Yamada–Janjic	Mellor–Yamada–Janjic	Bougeault and Lacarrère	Bougeault and Lacarrère

To evaluate the impact of high-resolution urban land cover databases in the mesoscale weather prediction models, a project called the National Urban Database and Access Portal Tool (NUDAPT) was created to provide accurate urban data with the idea of improving the parameterization of UBL processes (Ching et al. 2009). In this database, information exists relative to urban morphology for more than 40 cities in the United States. An advantage of using NUDAPT is that the inputs of the urban parameterizations (urban fraction, building height histograms, building plan area fraction, mean building height weighted by footprint plan area, etc.) are provided with a resolution of 1 km^2 and do not need to be defined for every urban class. This approach permits to exploit the whole urban information available for the city and consequently it is not limited by the number of urban classes. In the second part of this article, results obtained by running WRF with the urban canopy parameters (UCPs) derived from NUDAPT are compared to those previously obtained with the three urban classes derived from NLCD. Because the BULK scheme does not use urban morphological parameters, and the UCM is not yet ready to directly use the urban information from NUDAPT, only the BEP and BEP+BEM schemes were considered for this second comparison.

In section 2, a description of the simulations and the results for the four urban models are presented. Results obtained using the more detailed urban database (NUDAPT) are shown in section 3 for the BEP and BEP+BEM schemes. Section 4 explores the possibilities of the new BEP+BEM parameterization and the impact of the AC systems and their energy consumption. Conclusions and future directions are included in section 5.

2. WRF simulations with different urban models

a. Numerical domain and setup of the simulations

Two summer days have been analyzed: 25 and 31 August 2000. The 24-h simulations began at 1200 UTC (0600 LST) and a set of 8 simulations (4 urban schemes for every selected day) were performed using the nonhydrostatic version of the WRF V3.1 model (Skamarock et al. 2008), coupled to the Noah land surface model (Chen and Dudhia 2001; Ek et al. 2003) for the nonurban part. This surface-hydrology model has one canopy layer and the following prognostic variables: soil moisture and temperature in the soil layers, water stored in the vegetation canopy, and snow stored on the ground. The horizontal domain (see Fig. 1) was composed of four two-way nested domains with 100×100, 174×156, 219×186, and 216×198 grid points, and grid spacings of 27, 9, 3, and 1 km, respectively. The 24-h simulations were conducted with the initial and boundary conditions from the operational National Centers for Environmental Prediction (NCEP) with a grid resolution of 40 km and a time resolution of 3 h. To take full advantage of the urban parameterizations, a vertical resolution of 40 eta levels[1] was used (14 levels in the lowest 1.5 km; model top at ~20 km AGL) with the depth of the lowest level of approximately 22 m above the ground. The selected radiation parameterizations were the Dudhia (1989) shortwave radiation scheme and the Rapid Radiative Transfer Model (RRTM) longwave parameterization (Mlawer et al. 1997). The microphysics package is the WRF Single-Moment 3-Class Microphysics Scheme (WSM3; Hong et al. 2004); no cumulus cloud scheme was used in the inner domain. Two different PBL schemes were chosen, the Mellor–Yamada–Janjic (MYJ) scheme (Janjic 1994) for the BULK and UCM parameterizations and the Bougeault and Lacarrère (1989) for the BEP and BEP+BEM schemes. This selection is motivated by the fact that the first two parameterizations (BULK and

[1] Full eta levels = 1, 0.9974, 0.9940, 0.9905, 0.9850, 0.9800, 0.9700, 0.9600, 0.9450, 0.9300, 0.9100, 0.8900, 0.8650, 0.8400, 0.8100, 0.7800, 0.7500, 0.7100, 0.6800, 0.6450, 0.6100, 0.5700, 0.5300, 0.4900, 0.4500, 0.4100, 0.3700, 0.3300, 0.2900, 0.2500, 0.2100, 0.1750, 0.1450, 0.1150, 0.0900, 0.0650, 0.0450, 0.0250, 0.0100, and 0.0000. The vertical coordinate eta is defined as $(p - p_{top})/(p_{surf} - p_{top})$, where p is the dry hydrostatic pressure, p_{surf} is surface dry hydrostatic pressure, and p_{top} is a constant dry hydrostatic pressure at model top.

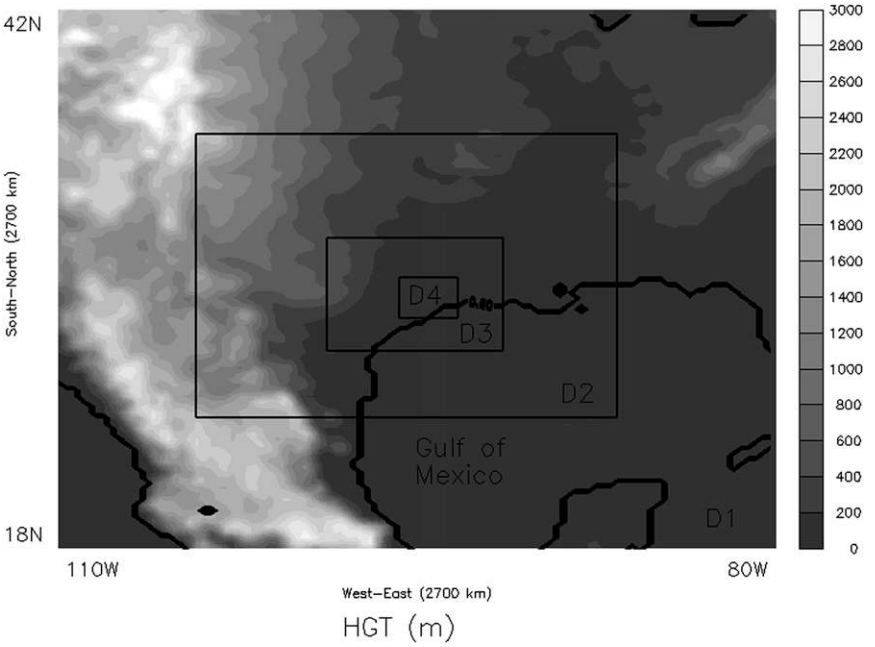

FIG. 1. Configuration of the four two-way nested domains for the WRF simulations. The grid sizes for the four domains are 27, 9, 3, and 1 km, respectively. Terrain height interval is 200 m.

UCM) have been extensively tested coupled to the MYJ scheme (e.g., Liu et al. 2006; Miao et al. 2009), while the other two (BEP and BEP+BEM), even if they can also be run with the MYJ scheme, have been mainly tested together with the Bougeault and Lacarrère (1989) PBL scheme (Martilli et al. 2003). We are aware that this choice may introduce another source of differences, but we considered that these are the configurations where each scheme can perform best. Future work will be needed to investigate the sensitivity of the urban parameterizations to the coupling with different PBL schemes.

In the determination of the fluxes provided by the urban canopy parameterization to the atmospheric models, the fractional area occupied by impervious surfaces (urban fraction) plays a fundamental role. The urban fraction (λ_U) in a particular patch is defined as the fractional area covered by the buildings λ_P (building plan area fraction) plus the fractional area covered by the roads. These parameters are especially important because they are used to obtain the dimensions of the buildings and roads in the urban schemes. For example, for a 2D urban canopy parameterization,

$$\frac{\lambda_P}{\lambda_U} = \frac{b}{b+w}, \tag{1}$$

where b and w are the widths of the buildings and roads, respectively. Other morphological urban parameters used to derive the inputs of the urban models are the mean building height weighted by building plan area $\overline{h}$ and the building height-to-width ratio $\overline{\lambda}_S$. These parameters are calculated using the following equations:

$$\overline{h} = \frac{\sum_{i=1}^{N} A_i h_i}{\sum_{i=1}^{N} A_i} \quad \text{and} \quad \overline{\lambda}_S = \frac{\overline{h}}{\overline{w}}, \tag{2}$$

where A_i is the plan area at ground level of building i, h_i is its height, N is the number of buildings, and $\overline{w}$ is the mean road width. In the simulations, the values of the above parameters used for every urban class for the city of Houston were extracted from the reports of Burian and Han (2003) and Burian et al. (2003) and can be seen in Table 2. Moreover, for the correct performance of the BEP and BEP+BEM schemes, a building height distribution is necessary for every urban class, and the considered values are in Table 2. The thermal properties of the buildings used in the simulations are in Table 3. For the UCM a diurnal profile of AH was added to the sensible heat flux (hereafter this simulation is referred as UCM+AH) with peak values of 90, 50, and 20 W m^{-2} for the commercial or industrial (COI), high-intensity residential (HIR), and low-intensity residential (LIR) urban classes, respectively. Unlike the UCM parameterization, the BEP+BEM scheme computes the AH released into the atmosphere to maintain the indoor temperature of the buildings in a range of comfort defined by the user

TABLE 2. Urban morphological parameters considered for the three urban classes.

	LIR	HIR	COI
Urban fraction (λ_U)	0.429	0.429	0.865
Building plan area fraction (λ_P)	0.06	0.17	0.21
Building height weighted by building plan area ($\overline{h}$) (m)	5.4	5.1	8.9
Building height-to-width ratio ($\overline{\lambda}_S$)	0.05	0.13	0.09
Buildings 5 m tall (%)	55	59	37
Buildings 10 m tall (%)	30	34	34
Buildings 15 m tall (%)	15	7	9
Buildings 20 m tall (%)	0	0	20

TABLE 3. Thermal parameters used in the urban modules (UCM, BEP, and BEP+BEM) and for every urban class [λ is the thermal conductivity of the material, C is the specific heat of the material, T(int) is the initial temperature of the material and also temperature of the deepest layer, ε is the emissivity of the surface, α is the albedo of the surface, and z_0 is the roughness length for momentum over the surface].

Surface	λ (W m^{-1} K^{-1})	C ($\times 10^6$ J m^{-3} K^{-1})	T (°C)	ε	α	z_0 (m)
Roof	0.695	1.32	20	0.9	0.2	0.01
Wall	0.695	1.32	20	0.9	0.2	—
Road	0.4004	1.40	20	0.95	0.15	0.01

(Salamanca et al. 2010) by means of an AC model that computes the total cooling loads for every floor of the buildings. For these simulations the amplitude of the range of comfort was fixed to 1°C with the target internal temperature being 25°C. Other parameters of the BEP+BEM scheme were fixed (for the three urban classes) to the coefficient of performance of the AC systems (COP) = 3.5, number of occupants = 0.02 person per meter squared of floor, and sensible heat generated by equipment = 30 W m^{-2} of floor from 0800 to 2000 LST and 10 W m^{-2} the rest of the day. The considered values for the sensible heat generated by equipment are similar to other estimations based on temporal variations of electric power consumption for lighting (Kikegawa et al. 2003) in business districts.

b. Analysis of the results

Houston is an area subject to complex mesoscale dynamics leading to complex land and sea breeze patterns. The main forcings determining the circulation are the contrast between the land and the sea and the general circulation patterns. The urban area intervenes, modulating these forcings. Given the purpose of this article, in the following analysis stress is put mainly on the impact of the urban forcing.

1) AIR TEMPERATURE

Table 4 lists the nine monitoring stations used in the evaluation of the four urban models for the two selected days. The stations were displayed over the city of Houston; their locations can be seen in Fig. 2b. The stations selected are representative of the three urban classes considered in this study, so that the behavior in simulating urban areas with different morphology can be analyzed. It is important to remember that we assume that point measurements can be compared to model outputs, which represent spatially averaged values over a grid cell of 1 km^2. An analysis of this assumption requires detailed information on the position of the station and the morphology of the surrounding area and goes beyond the scope of this work.

The inner simulation domain is plotted in Fig. 2a. The observed and computed statistics for the 2-m air temperature are shown in Tables 5 and 6. Mean bias (MB), hit rate (HR), and root-mean-square error (RMSE) were calculated with the criteria for the HR calculation for model–observation agreement within 2°C following the criteria of similar studies (Miao et al. 2009). It is important to mention, in terms of the comparison, that the observed values are hourly averaged data whereas no time average of WRF outputs was performed. The four urban schemes reproduce accurately enough (HR $>$ 0.5 for all the stations) the surface air temperature for 25 August (see Fig. 3 and Table 5). The best results were obtained with the BEP+BEM and BULK schemes. The BULK parameterization tends to slightly overestimate the air temperature (the MB is almost always positive) whereas the other schemes tend to underestimate it. Observing the differences in the air temperature between the two multilayer schemes (BEP and BEP+BEM), it is possible to say that the effect of the sensible heat ejected into the atmosphere to maintain the indoor temperature in a range of comfort (situation simulated with the BEP+BEM scheme) has a significant effect from 1800–1900 LST to dawn. In general, the worst estimations were obtained with the single-layer UCM+AH scheme,

TABLE 4. List of monitor locations based on information from Texas Commission on Environmental Quality (TCEQ). The urban morphology characteristics for every urban class can be seen in Table 2. Hereinafter ID indicates the identifier number for the site.

ID	Lat	Lon	Sampling height above ground (m)	Urban class
C01	29.767 778	−95.220 556	11	COI
C55	29.733 611	−95.257 500	5	HIR
C81	29.735 000	−95.315 556	11	HIR
C146	29.695 556	−95.499 167	4	LIR
C167	29.734 167	−95.238 056	11	HIR
C169	29.706 111	−95.261 111	11	LIR
C404	29.806 944	−95.291 389	11	HIR
C409	29.623 889	−95.474 167	11	HIR
C603	29.765 278	−95.181 111	4	COI

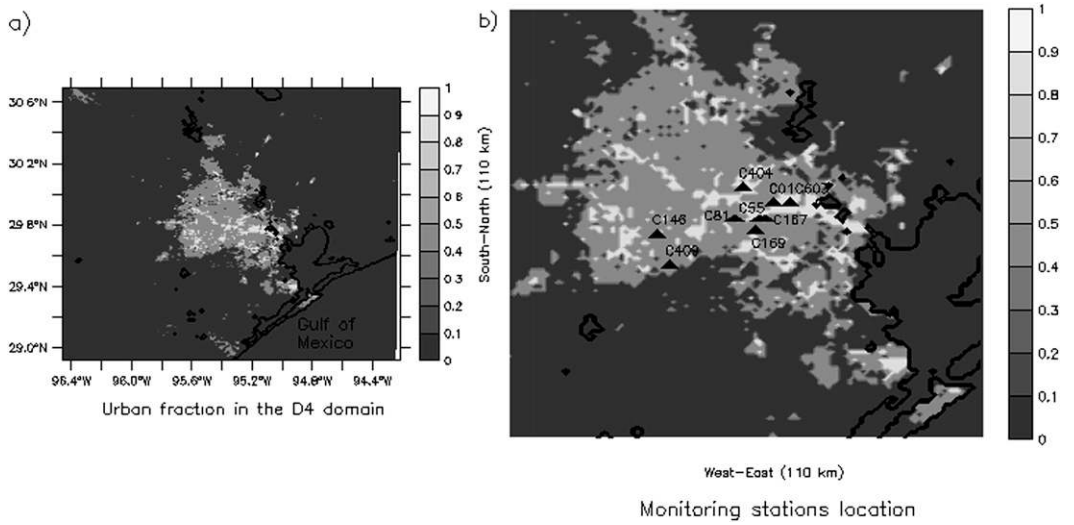

FIG. 2. (a) The D4 inner domain and urban fraction (from Table 2) for the city of Houston. (b) Monitoring stations used in the evaluation of the four urban parameterizations.

but they notably improved in the COI areas where the urban fraction (see Table 2) has the largest value. The warmest day was 31 August, with temperatures up to 41°C. The results (see Fig. 4 and Table 6) indicate a good performance of the urban models except for the UCM+AH scheme, which was not able to correctly simulate the surface air temperature from 1800 to 1900 LST except in the COI areas. We are aware that the UCM parameterization has been widely tested and validated (e.g., Kusaka and Kimura 2004; Lin et al. 2008; Miao et al. 2009) in different situations, so the results obtained for 31 August were probably due to the low urban fraction used for the HIR and LIR urban classes, which were derived from the available information on urban morphology. It seems that this is not a setback for the BEP and BEP+BEM parameterizations. At this point, it is important to remember that the goal of this work is twofold: on one hand, we want to compare the BULK, UCM, BEP, and BEP+BEM schemes coupled to the WRF model; on the other hand, we want to study the impact of using highly accurate urban morphology information on the meteorological variables with different urban canopy parameterizations. This is the reason why we use the realistic urban fraction (see Table 2) derived from the Burian and Han (2003) and Burian et al. (2003) reports for the different urban classes and not the values that give the best results.

2) WIND FIELD

In Fig. 5, the time evolution of the wind speed at 10 m above the ground level (AGL) is compared with the observations for 25 August. Three monitoring stations are shown because the others do not present remarkable differences. The four urban models were able to capture satisfactorily the rotation of the breeze (from the sea to the land and vice versa) from around 1400–1500 LST to dawn. The BULK and UCM+AH schemes slightly overestimate the wind speed compared to the BEP and BEP+BEM parameterizations, which underestimate the observed wind. It is important to remember that BULK and UCM+AH use a roughness length that is not directly dependent on the urban morphology, while BEP and BEP+BEM estimate the momentum sink with a drag force that depends of the urban morphology. During the first hours of the day, from sunrise to 1100 LST approximately, the schemes were not able to capture the wind direction well. Later, and for a period of some hours, the direction of the wind was changing randomly. This behavior was due to scattered clouds modeled over the city. The solar radiation does not heat the urban surface below the cloud, and consequently the air blows away to surrounding warmer areas. This phenomenon (not shown) was observed with the four urban schemes in different places and times.

It is interesting to analyze how the different surface schemes affect the cloud prediction. In Fig. 6 the shortwave radiation that reaches the ground (in the case of built-up areas, this is the shortwave radiation that reaches the upper limit of the urban canopy layer) is shown at 1200 LST. This field reflects the presence of clouds. It can be seen that, at that time, the simulations with the BEP and BEP+BEM schemes produce clouds above the city, while UCM and BULK do not. This is related to strong vertical velocities (Fig. 7) simulated by BEP and BEP+BEM. A few hours later, similar patterns (clouds and strong updrafts and downdrafts) developed also for the UCM and BULK simulations over the city. A possible explanation of

TABLE 5. Statistical comparison of the simulated and observed 2-m air temperature (°C; the criterion for hit rate calculation is 2°C) for 25 Aug 2000.

25 Aug 2000	BULK	UCM+AH	BEP	BEP+BEM	ID
MB	0.9441	−0.1846	−0.4477	−0.1146	C01
RMSE	1.0591	1.2252	1.3012	0.9174	
HR	0.9583	0.9167	0.8750	0.9583	
MB	1.0156	−0.7632	−0.6829	−0.1733	C55
RMSE	1.4369	2.3053	1.9029	1.4190	
HR	0.7917	0.6667	0.5833	0.8750	
MB	0.4996	−1.0780	−1.1773	−0.7023	C81
RMSE	0.8864	2.3070	1.7794	1.2975	
HR	1.0000	0.6667	0.7083	0.8750	
MB	0.9174	−0.7859	−0.7757	−0.2760	C146
RMSE	1.1352	1.6233	1.2510	0.8454	
HR	0.9583	0.8333	0.8750	1.0000	
MB	0.3214	−1.3697	−1.4086	−0.8324	C167
RMSE	1.3148	2.8136	2.4667	1.8656	
HR	0.8333	0.6250	0.5833	0.6250	
MB	1.4077	−0.3472	−0.2420	0.2936	C169
RMSE	1.6013	1.7647	1.2407	1.1344	
HR	0.7917	0.7500	0.8750	0.9167	
MB	−0.7305	−2.3791	−2.5281	−1.8296	C404
RMSE	1.1633	3.1474	2.9407	2.2238	
HR	0.9583	0.5417	0.4583	0.5000	
MB	−0.2036	−1.5205	−1.4305	−1.0776	C409
RMSE	1.1597	2.0500	1.6861	1.3535	
HR	0.9583	0.5417	0.6250	0.9167	
MB	0.3717	−0.4699	−1.0604	−0.4341	C603
RMSE	0.7086	0.9659	1.5736	0.8885	
HR	1.0000	0.9583	0.7500	1.0000	

TABLE 6. Statistical comparison of the simulated and observed 2-m air temperature (°C; the criterion for hit rate calculation is 2°C) for 31 Aug 2000.

31 Aug 2000	BULK	UCM+AH	BEP	BEP+BEM	ID
MB	0.7332	−0.6974	−0.8760	0.0400	C01
RMSE	1.2844	1.5344	1.7177	1.2112	
HR	0.8750	0.8333	0.6667	0.9583	
MB	0.4255	−2.1762	−0.9776	−0.2609	C55
RMSE	1.2351	3.6834	2.0046	1.5049	
HR	0.9167	0.4167	0.6250	0.7500	
MB	0.2226	−2.6085	−1.2804	−0.5661	C81
RMSE	1.0908	3.9160	2.0344	1.3927	
HR	0.9583	0.4167	0.5833	0.8750	
MB	0.9850	−1.8046	−0.7235	−0.0946	C146
RMSE	1.2923	3.3064	1.6357	1.2688	
HR	1.0000	0.6667	0.7500	0.9167	
MB	0.4296	−2.1180	−1.0245	−0.2328	C167
RMSE	1.1569	3.1247	1.6067	1.1472	
HR	0.9167	0.5417	0.8333	0.8750	
MB	0.9149	−1.9793	−0.6860	−0.1065	C169
RMSE	1.3409	3.2054	1.3515	1.1006	
HR	0.9167	0.4583	0.8750	0.9167	
MB	−1.4044	−4.0587	−3.0171	−2.0374	C404
RMSE	1.7845	4.8135	3.3670	2.2620	
HR	0.7500	0.2917	0.2500	0.4583	
MB	0.5148	−1.6033	−0.7080	−0.1324	C409
RMSE	1.4530	3.1778	1.8077	1.6253	
HR	0.8750	0.6667	0.7083	0.7083	
MB	0.1513	−0.3021	−1.2128	−0.0001	C603
RMSE	1.0279	1.1052	1.6225	0.9693	
HR	1.0000	0.9167	0.7917	1.0000	

these differences is that BEP and BEP+BEM are more sensitive to the spatial variability of surface fluxes because of the heterogeneity of the urban structure. For this reason they trigger earlier the updrafts and downdrafts that are responsible for cloud formation. It is difficult (and goes beyond the scope of this article) to decide which is the most realistic behavior not only because there are no cloud position and formation measurements available during these days over Houston, but also because this problem involves an analysis of the behavior of the PBL and cloud schemes (one of the weakest areas of meteorological models). At this stage, the influence of the urban parameterization on cloud formation is only a speculation. Further studies should be dedicated to analyze if the models' predictions are accurate, if they are influenced by incorrect parameterization of the physics of the phenomena or by numerical noise.

On 31 August, the wind blew from the northwest over Houston during the morning until approximately 1300 LST. Simulations with different urban schemes were able to capture this flow well, but the presence of clouds some hours later made impossible the correct prediction of the wind field at the monitoring locations after midday. In the evening and during all the night, the schemes captured the clockwise turn of the breeze well (not shown).

In Fig. 8, vertical wind speed profiles (together with the PBL height predictions) are compared against observations at Ellington Place for 25 August. The four schemes present similar patterns for the wind field with a shift in direction in the lower levels compared to the observed values. In Fig. 9 the PBL heights forecast by the four schemes against observations have been plotted for the Ellington and Southwest Airport locations. The BULK scheme predicts the highest values and the BEP+BEM scheme the lowest. It must be noted, however, that all models computed strong spatial heterogeneities for this field over the entire inner domain (not shown).

3. WRF simulations with the NUDAPT data

a. Setup of the simulations

Lo et al. (2007) show that an up-to-date urban land use–cover dataset and an urban scheme able to distinguish the heterogeneities present in the cities have a significant impact on mesoscale simulations of the urban

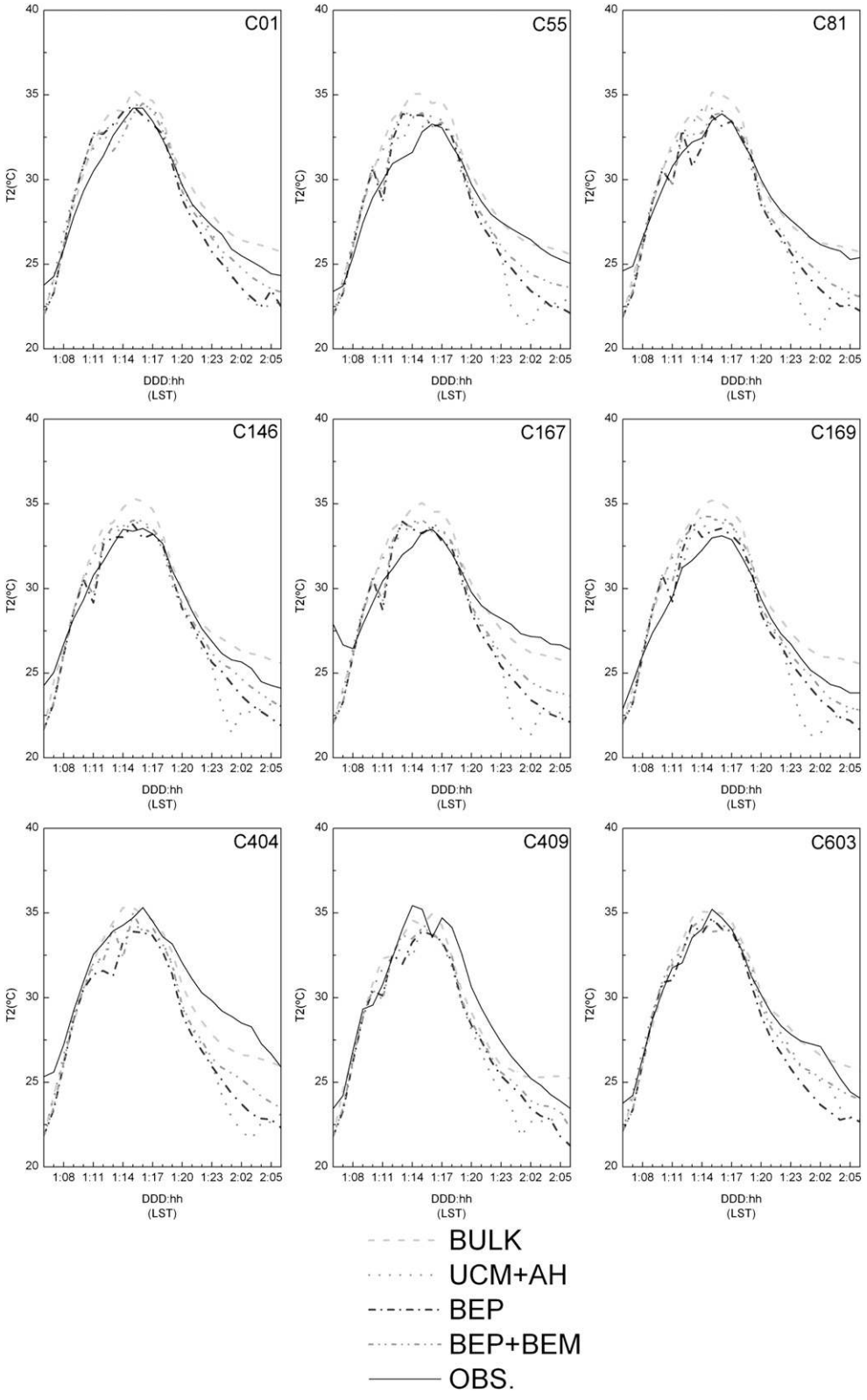

FIG. 3. Time series of 2-m air temperature for different stations for 25 Aug 2000 obtained with the four urban schemes against measurements.

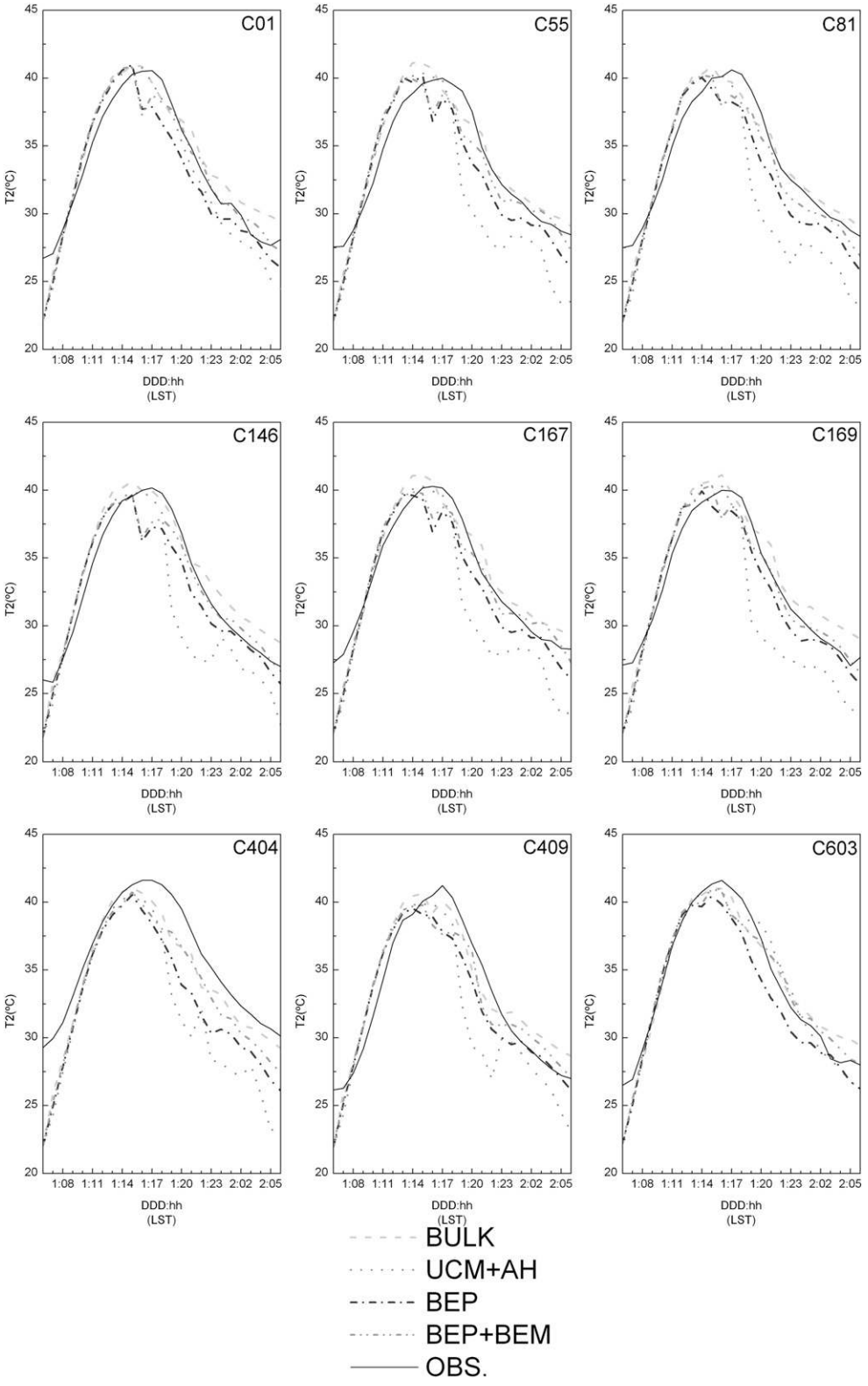

FIG. 4. As in Fig. 3, but for 31 Aug 2000.

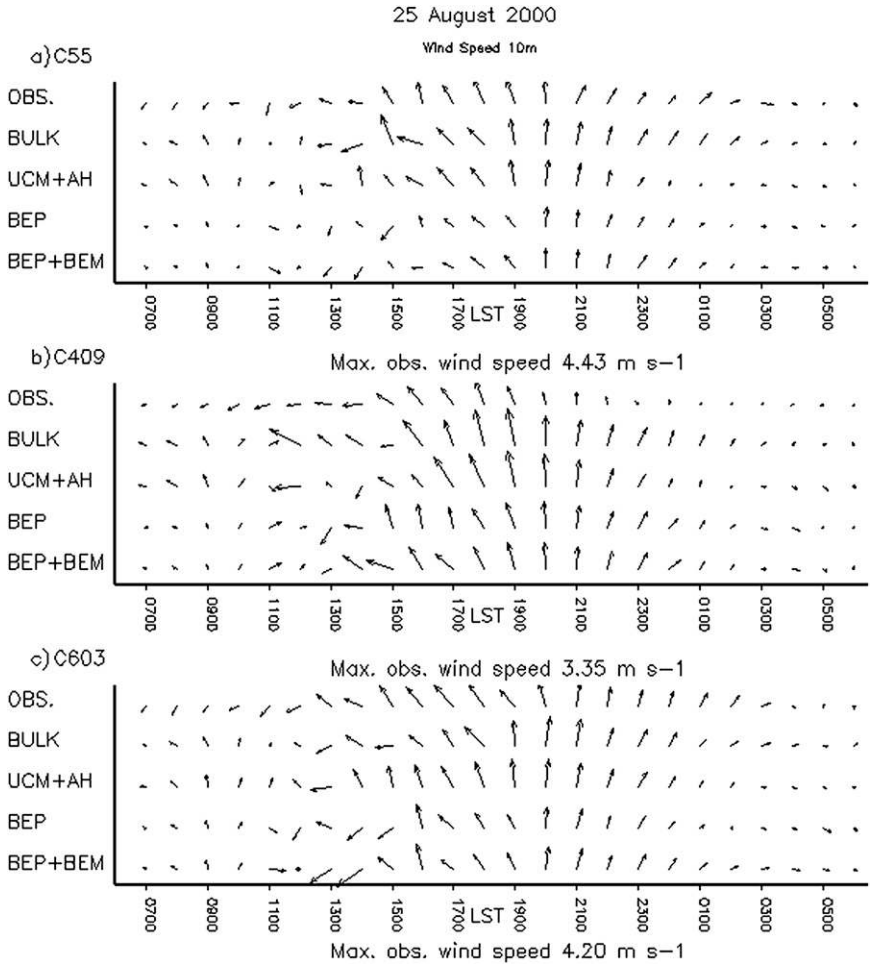

FIG. 5. Time series of observed (OBS) and simulated (with the four urban schemes) horizontal winds at 10 m AGL at 3 sites for 25 Aug: stations (a) C55, (b) C409, and (c) C603.

environment of Pearl River Delta region in China. Other studies (e.g., Sertel et al. 2010) also reflect the importance of using accurate land cover data to predict the air temperature on regional climate simulations.

On this line, we have analyzed the impact of a high-resolution urban canopy parameter database on the simulation of the UBL over Houston. For this purpose, the information existing in NUDAPT for the city of Houston and surrounding areas was analyzed. The following gridded urban morphological parameters of a region that covers 5242 km^2 were considered as input for the urban parameterizations: urban fraction, building height histograms, building plan area fraction, building height weighted by footprint plan area, and building surface area to plan area ratio (λ_B), where λ_B is defined as the sum of building surface divided by the total plan area of the study location. All these parameters with a resolution of 1 km^2 were introduced as new variables in the input files of the WRF model. In an urban grid point, then, the urban schemes use the information from the NUDAPT database and not the averaged properties defined in Table 2. The numerical domains and physics setup are equal to those used for the previous simulations.

b. *Analysis of the results*

1) AIR TEMPERATURE

To evaluate the impact of gridded NUDAPT data on the 2-m air temperature, the RMSEs (NUDAPT) were computed and compared with the previous RMSEs (urb_class). The term urb_class hereinafter refers to the simulations that use the input parameters of Table 2 for every urban class. To quantify the comparison, the relative difference ΔT2 was calculated

$$\Delta T2 = 100 \times \frac{\mathrm{RMSE(urb\_class)} - \mathrm{RMSE(NUDAPT)}}{\mathrm{RMSE(urb\_class)}} \quad (3)$$

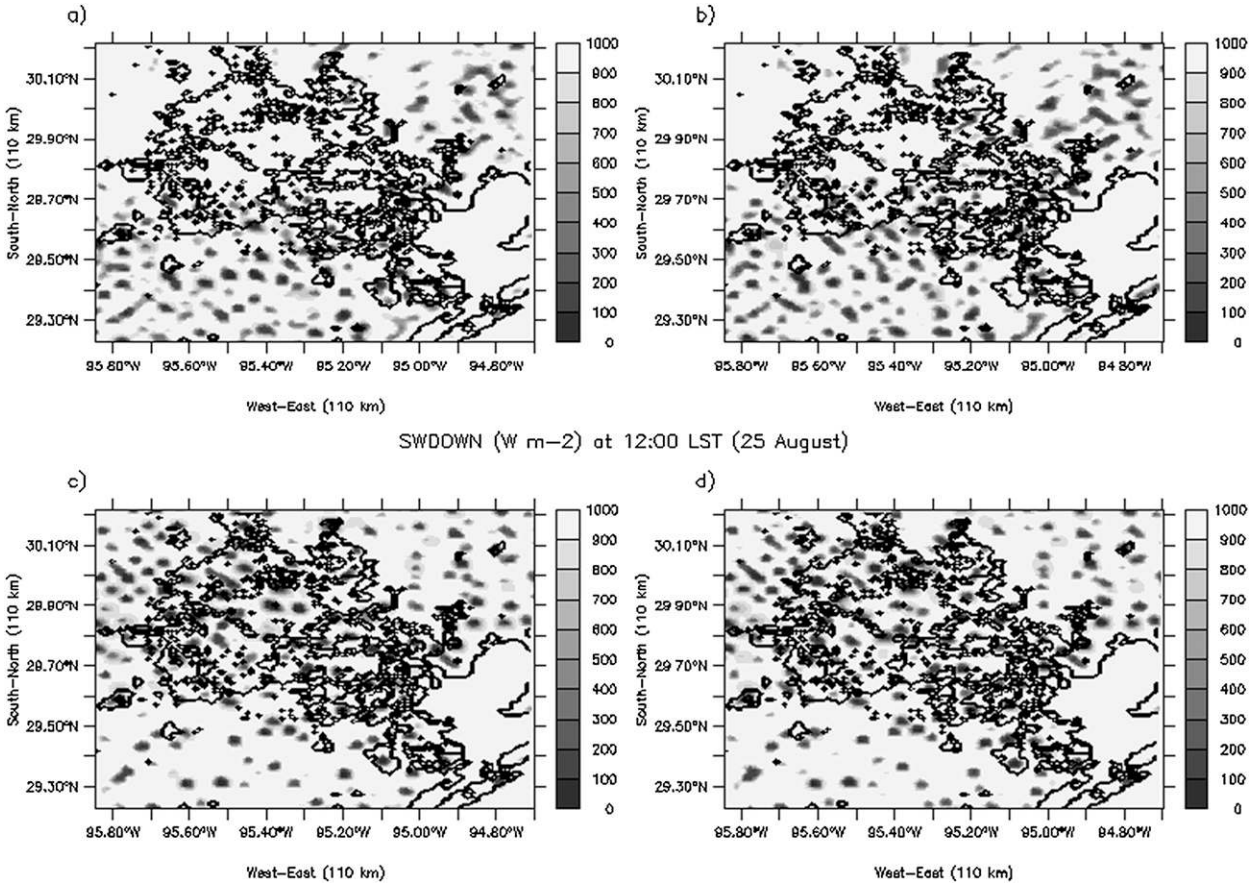

FIG. 6. Shortwave downward radiation (W m^{-2}) reaching the ground obtained with the four urban models at 1200 LST 25 Aug 2000: the (a) BULK, (b) UCM+AH, (c) BEP, and (d) BEP+BEM schemes.

for every monitoring station and day simulated. A positive value means an improvement in the results and a negative value the opposite. The ΔT2 values obtained are presented in Table 7, and the differences between the observation and model predictions are plotted in Figs. 10 and 11. In this comparison, 13 negative against 23 positive values for the relative difference ΔT2 were obtained. It is not easy to observe a clear tendency looking at Table 7, except that the BEP+BEM scheme seems to present a greater sensibility to the urban morphology parameters than the BEP parameterization. This fact can be understood because the BEP+BEM scheme computes the AH released into the atmosphere to maintain the indoor temperature in a range of comfort, and this heat flux is strongly dependent on the urban fraction and the dimensions of the buildings. On the other hand, in the BEP scheme the indoor surface-wall temperature is fixed during the whole simulation and no anthropogenic heat flux is directly ejected into the atmosphere. It is important to mention that after 1900 LST and during all the night, the sign of the air temperature difference between the BEP+BEM (NUDAPT) and BEP+BEM (urb_class) simulations is kept constant (positive or negative) in most of the stations, which would mean that the AH released during all the day (which in this case has a strong dependence on the urban geometry) is an important component of the nocturnal UHI phenomenon. This behavior is less significant when the BEP (NUDAPT) and BEP (urb_class) simulations are compared, given that the AH is not taken into account. These results suggest that the urban fraction and the AH are important factors that contribute to the UHI. The urban geometry is less important and becomes relevant because it affects the AH. In Fig. 12 the 2-m air temperature differences [T2(NUDAPT) − T2(urb_class)] for the BEP+BEM parameterization are plotted for the two days simulated at 0300 LST (when the differences are maximal). These differences are smaller with the BEP scheme (not shown), especially for 25 August (the colder day). On 31 August, the surface air temperature is slightly overestimated during the night when the NUDAPT information is used with

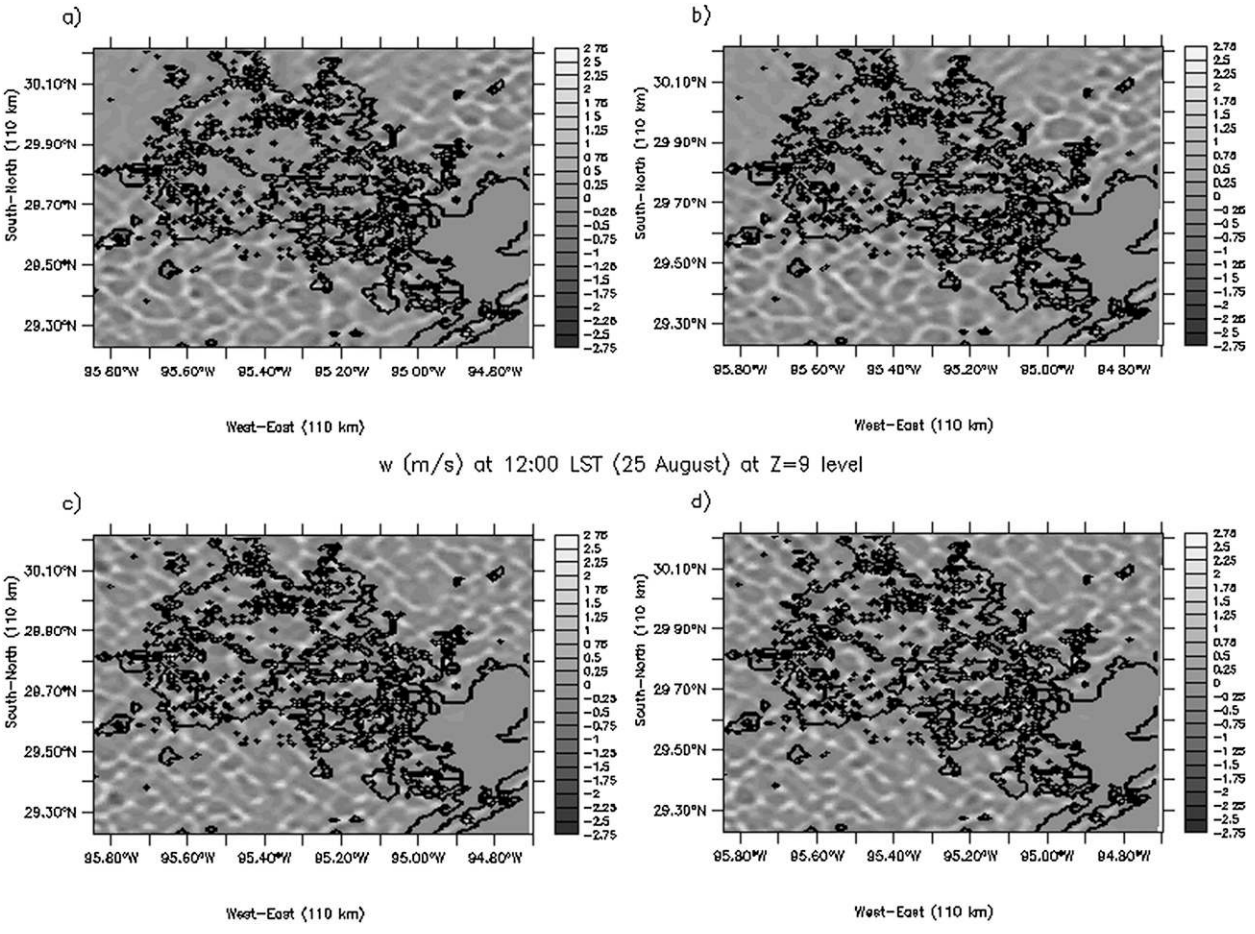

FIG. 7. Vertical velocity (m s^{-1}) patterns obtained with the four urban models at 1200 LST 25 Aug 2000 at eta level $Z = 9$ ($\approx$ 485 m): (a) BULK, (b) UCM+AH, (c) BEP, and (d) BEP+BEM.

the BEP+BEM scheme (see Fig. 11). More simulations are needed to study the sensitivity to the target temperature and range of comfort. Without a larger number of monitoring stations well distributed over the city and without more days simulated, it is difficult to extract definitive conclusions from this comparison. With the information available, it is possible to say that the BEP scheme is less sensitive to the urban morphology for surface air temperature predictions than the BEP+BEM scheme because the AH is strongly dependent on the urban morphology of the city. This is because, in a certain sense, the AH resulting from air conditioning is proportional to the number of floors.

2) WIND FIELD

In Fig. 13, the wind speed at 10 m AGL is compared with the observations for 25 August in three monitoring stations (the rest of the stations did not show remarkable differences). It is difficult to highlight some conclusion from this comparison because the wind field is very influenced by the presence of clouds, and when the NUDAPT information is used the position of the clouds is modified with respect to the urb_class simulation. Nevertheless, it shows the impact of using different urban morphology data on the cloud prediction. When there were no clouds the wind field was captured reasonably well both days. In Fig. 12, together with the air temperature differences, the wind speed differences have been plotted (NUDAPT minus urb_class simulation). The fact that the vectors point from the region where NUDAPT simulated colder temperature toward those where it simulated hotter temperatures means that the use of realistic NUDAPT data for the morphology of the city of Houston increased the convergence of the flow above the hotter downtown area, at least for the days simulated.

4. Waste heat emission and energy consumption

In the last part of this article, the total energy consumption (EC) due to air conditioning has been analyzed

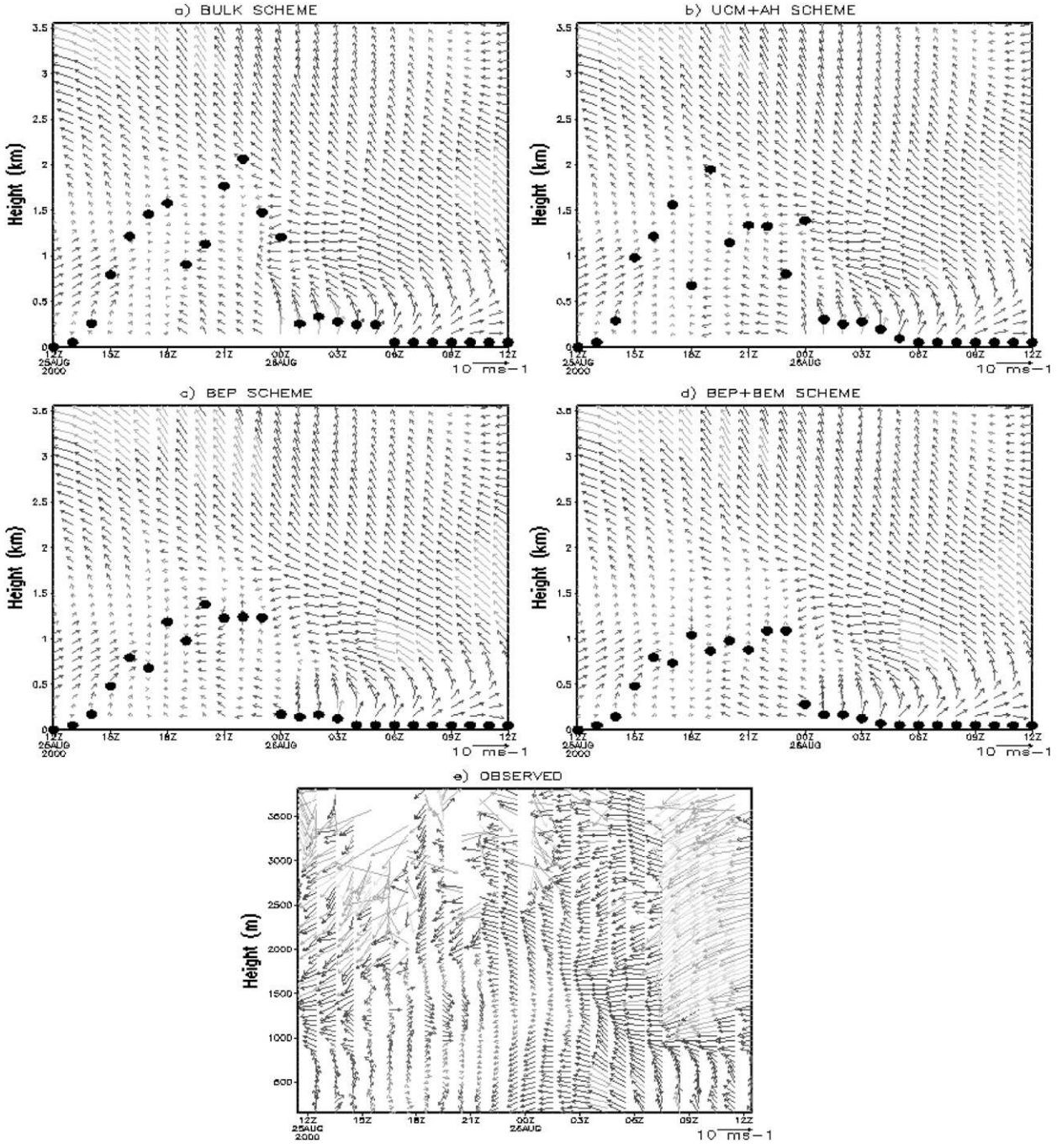

FIG. 8. Vertical wind speed (m s^{-1}) profiles [together with the PBL height (km) predictions] for 25 Aug 2000 (UTC = LST + 6 h) at Ellington Pl for (a) BULK, (b) UCM+AH, (c) BEP, (d) BEP+BEM, and (e) observations.

with the BEP+BEM scheme (the only scheme that allows this calculation). The value of instantaneous energy consumption ec(x, y, t) (W m^{-2}) due to the space cooling–heating is computed in this parameterization at every urban grid point, and the total consumption can be computed as following:

$$\mathrm{EC} = \int_0^T \left(\iint_{\substack{\text{urban} \\ \text{domain}}} \mathrm{ec}\, dx\, dy \right) dt, \tag{4}$$

where T is the period of simulation.

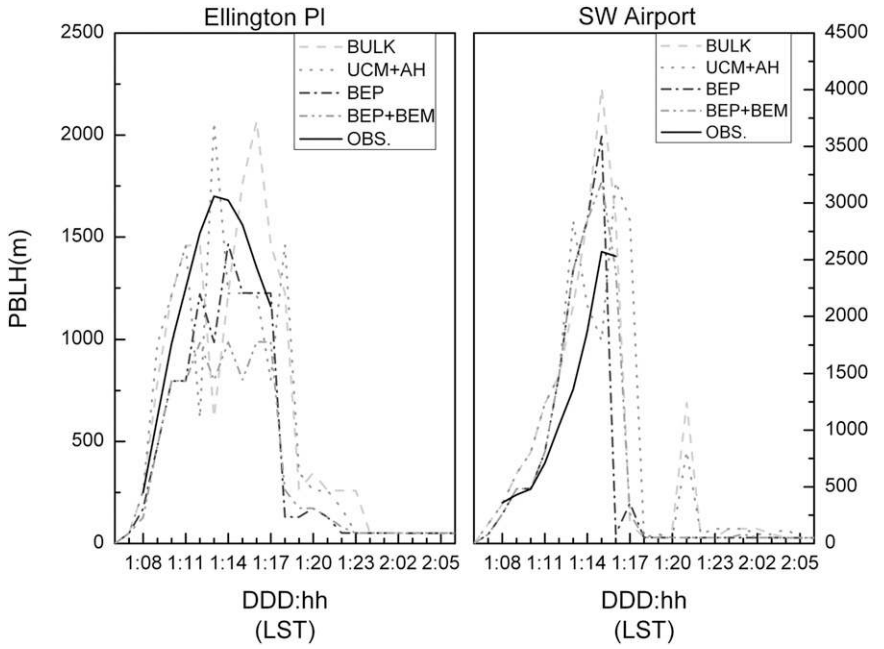

FIG. 9. The PBL height computed against observed at (left) Ellington and (right) Southwest Airport for 25 and 31 Aug 2000, respectively.

In BEP+BEM, all the buildings are considered of the same type (only the dimensions can be different), and all the buildings in the domain are assumed to run the AC. Taking this into account, the EC was calculated considering the high-resolution urban canopy parameters dataset (NUDAPT) and the urban class classification for the 2 days simulated. The EC (NUDAPT) for 25 August over the whole domain was of 197 347 MW h, while for EC (urb_class) it was 13.6% higher. For 31 August, the EC (NUDAPT) over the whole domain was 251 419 MW h whereas for EC (urb_class) it was 8.9% higher. The differences in the EC due to the different meteorological conditions between the two selected days were 21.5% and 17.2% for the NUDAPT and urb_class cases, respectively. Heiple and Sailor (2008) estimated the daily averaged energy consumption from all sources (space cooling, lighting and appliances, and water heating) for the city of Houston for the month of August with top-down and bottom-up approaches as 108 588 and 105 869 MW h, respectively. It is difficult to compare these results since the urban area considered by Heiple and Sailor (2008) is only a fraction of the urban area considered in our simulation domain. To get a more meaningful comparison, the energy consumption in the grid points classified as commercial (based on the NLCD database) was computed and compared with those obtained by Heiple and Sailor (2008) for the commercial areas (see Table 8). The following sources of uncertainty must be kept in mind when comparing these results:

- The values computed by Heiple and Sailor (2008) account for the total energy consumption (not only AC, but also lighting and water heating), while those computed in our simulation are only due to AC. Nationally, 45% of the annual energy consumed in commercial buildings is for space cooling (or heating).

TABLE 7. Relative difference errors ΔT2 obtained for every monitoring station and day analyzed. The relative difference errors are derived using the following equation: $\Delta T2 = 100 \times [\text{RMSE(urb\_class)} - \text{RMSE(NUDAPT)}]/\text{RMSE(urb\_class)}$.

Monitoring stations	25 Aug 2000 ΔT2 (%)	31 Aug 2000 ΔT2 (%)	Urban parameterization
C01	0.0836	2.2184	BEP
	13.8690	8.5102	BEP+BEM
C55	12.0632	9.6690	BEP
	23.8582	10.5053	BEP+BEM
C81	11.1394	13.0313	BEP
	30.2381	−0.9771	BEP+BEM
C146	−4.3597	21.8200	BEP
	−4.0040	21.1580	BEP+BEM
C167	6.9939	9.8589	BEP
	14.8666	−8.9933	BEP+BEM
C169	5.3486	12.9915	BEP
	−6.2806	−54.9167	BEP+BEM
C404	6.1292	1.4235	BEP
	12.0630	9.5851	BEP+BEM
C409	−3.7719	−1.3133	BEP
	−4.4652	4.7144	BEP+BEM
C603	−21.9458	−42.2202	BEP
	−43.8009	−52.9864	BEP+BEM

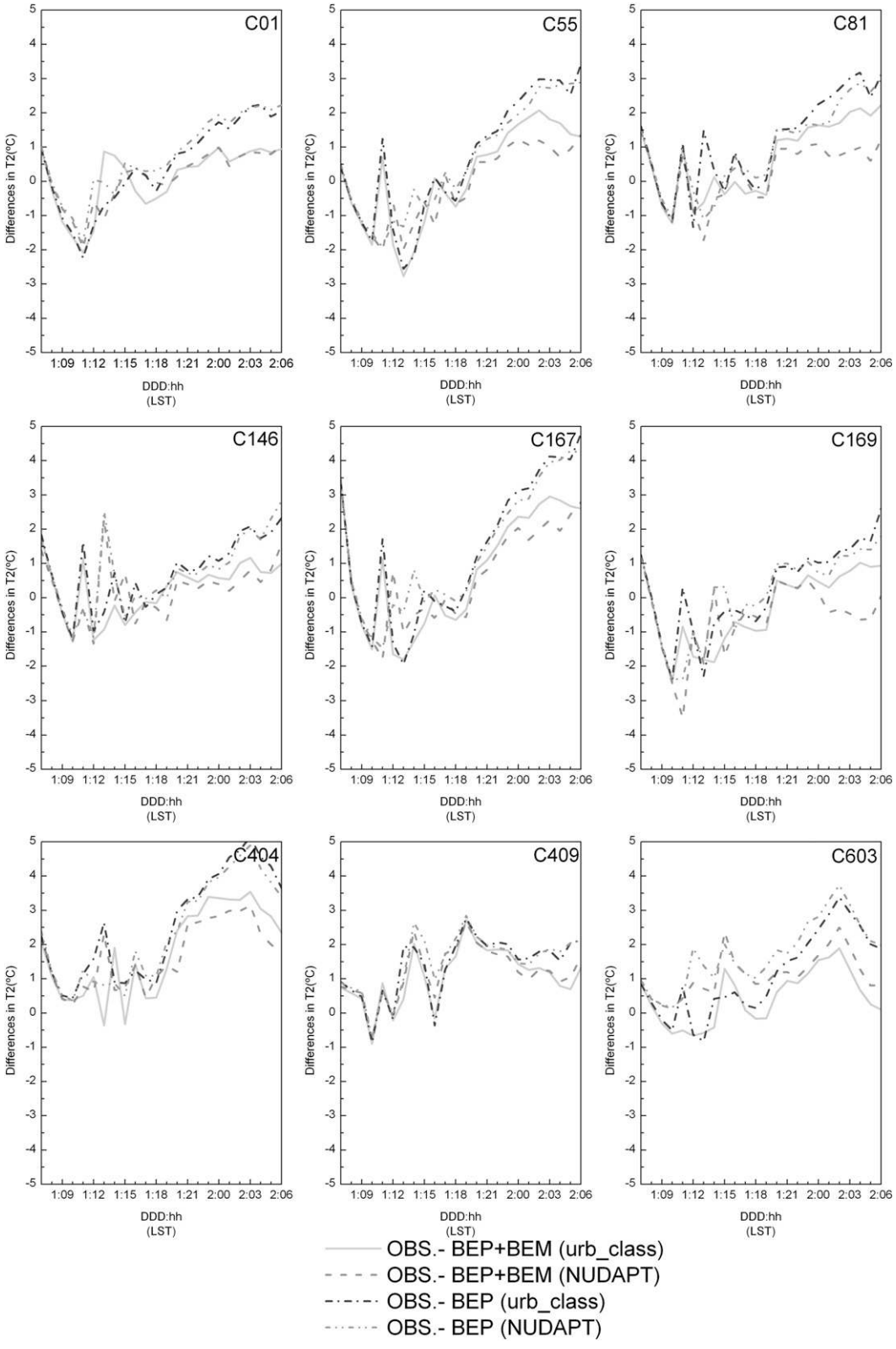

FIG. 10. Differences between the observed and computed 2-m air temperature for 25 Aug 2000 for different stations.

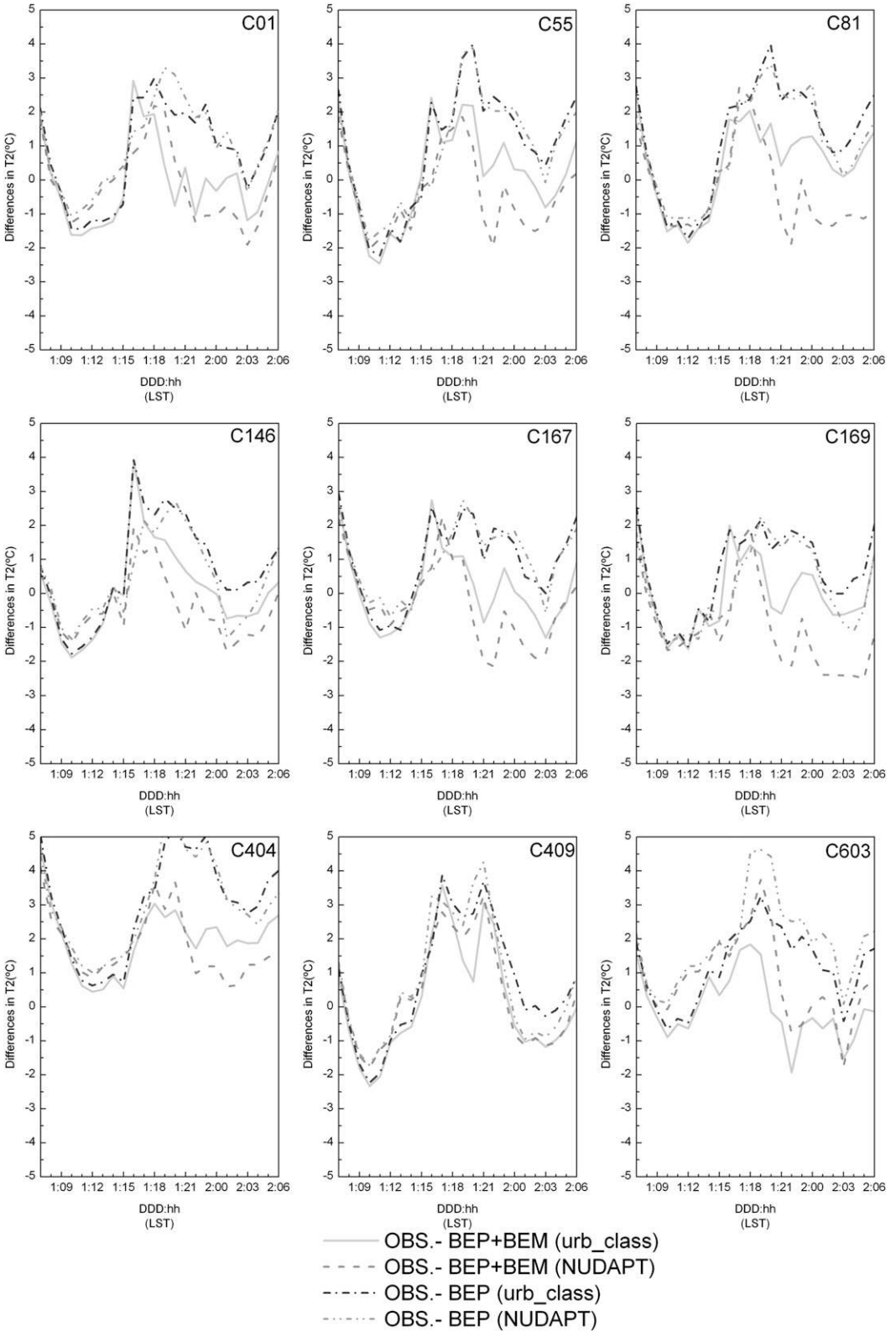

FIG. 11. As in Fig. 10, but for 31 Aug 2000.

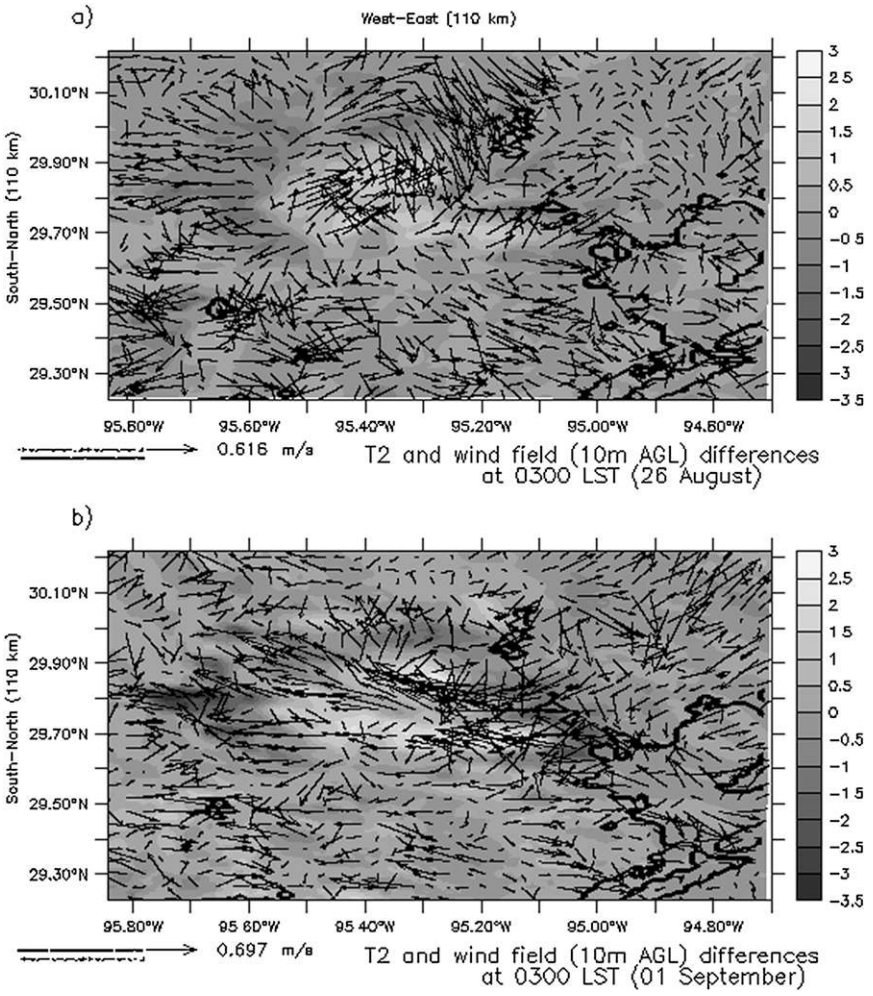

FIG. 12. (a) The 2-m air temperature differences [T2(NUDAPT) − T2(urb_class)] (°C) and wind speed (at 10 m AGL) differences (m s^{-1}) at 0300 LST (26 Aug) obtained with the BEP+BEM scheme. (b) As in (a), but at 0300 LST (1 Sep).

If this proportion is valid also for the days simulated, it can be concluded that the model overestimates the energy consumption by a factor of 1.7–2.2 for NUDAPT and a factor of 3–4 for urb_class. It is likely, however, that for the summer days considered the fraction of energy used for AC was larger than 45% and the overestimation lower.

- It is assumed that the points classified as commercial in the NLCD data belong all to the city of Houston and that they overlap with the points considered as commercial in the work of Heiple and Sailor (2008). With the information in our possession it is not possible to verify this assumption. By a simple visual analysis of a map of the city it can be seen that although the majority of commercial areas are located within the city limits, there are commercial points outside, in particular in the southern part of the domain (e.g., Galveston area). This may partially explain the larger energy consumption obtained by the model.
- The values computed by Heiple and Sailor (2008) are daily averages based on climatic data for the month of August, whereas our simulations were done for two specific days (25 and 31 August 2000). The second of them (31 August), in particular, was significantly hotter (maximum temperature 41°C) than the monthly average values (average maximum temperature for the month of August in Houston was 33°C for this year). It is likely then that the energy consumption for AC was higher than the monthly average values.

Indeed, some refinements must be done in the BEP+BEM parameterization to correct this overestimation in the energy consumption—for example, by considering different typologies of buildings that may use different

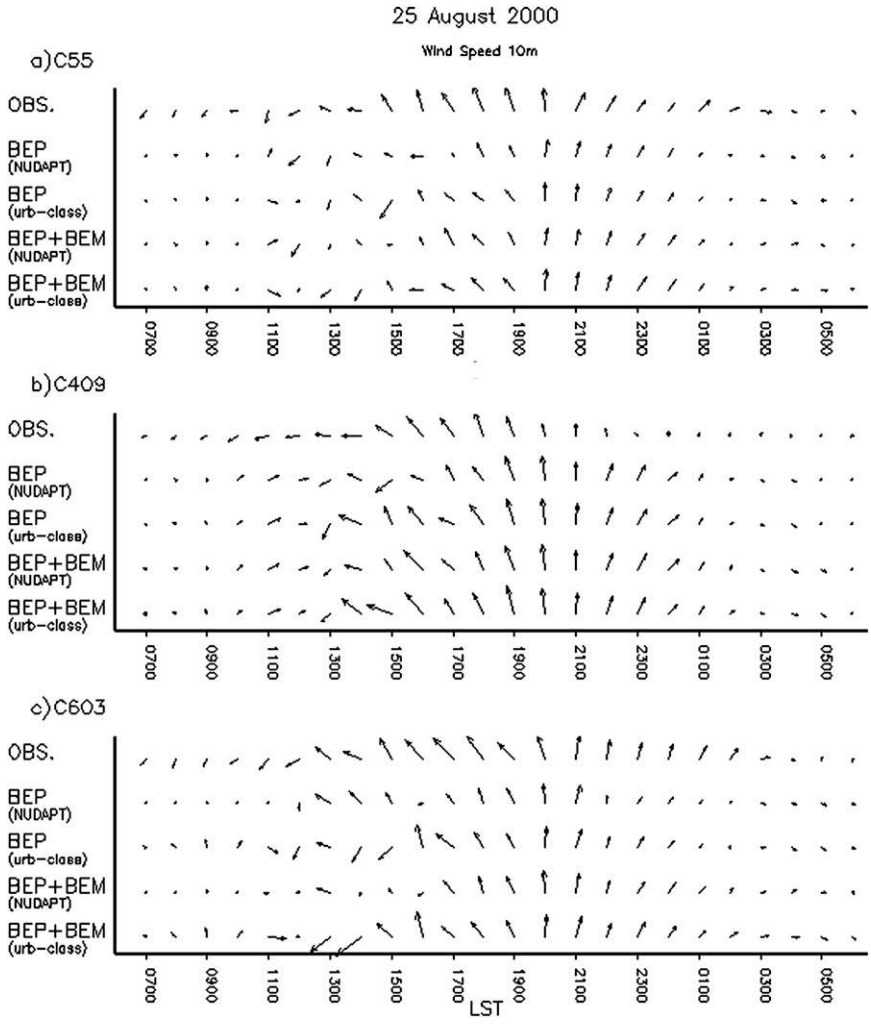

FIG. 13. Time series of observed (OBS) and simulated (with BEP and BEP+BEM schemes) horizontal winds at 10 m AGL for 25 Aug at three sites: stations (a) C55, (b) C409, and (c) C603.

types of AC (or no AC at all). To do this, state-of-the-art building energy models (e.g., DOE 2005) can help significantly to improve the performances of BEP+BEM. These models, more sophisticated than BEM, are built to evaluate the energy consumption of a single building and are not linked to an atmospheric model but they use climatological data. However, taking into account also the limitations of an urban canopy parameterization (some of them mentioned previously in this section) with respect to the top-down and bottom-up methodologies, we think that the results are a good starting point to create a tool that can give reasonable estimates of energy consumption without the need of very detailed information describing each building, which is often difficult to obtain. Another interesting conclusion that can be derived from these results is that the total energy consumption is very sensitive to the urban database used. Detailed information on the urban morphology is necessary (like that in NUDAPT) to get a realistic estimate of the energy consumption.

Finally, the impact of the AH on the air temperature has been addressed. For this purpose, four new simulations with the BEP+BEM scheme were performed, where the AH coming from the AC systems was not ejected into the air. In Figs. 14 and 15, the 2-m air temperature differences have been plotted for the two

TABLE 8. Daily energy consumption computed by the model and estimated by Heiple and Sailor (2008) with the top-down and bottom-up techniques.

Daily energy consumption (MW h)	NUDAPT	Urb_class	Top down	Bottom up
25 Aug	34 946	66 790	45 853	45 483
31 Aug	45 058	80 660		

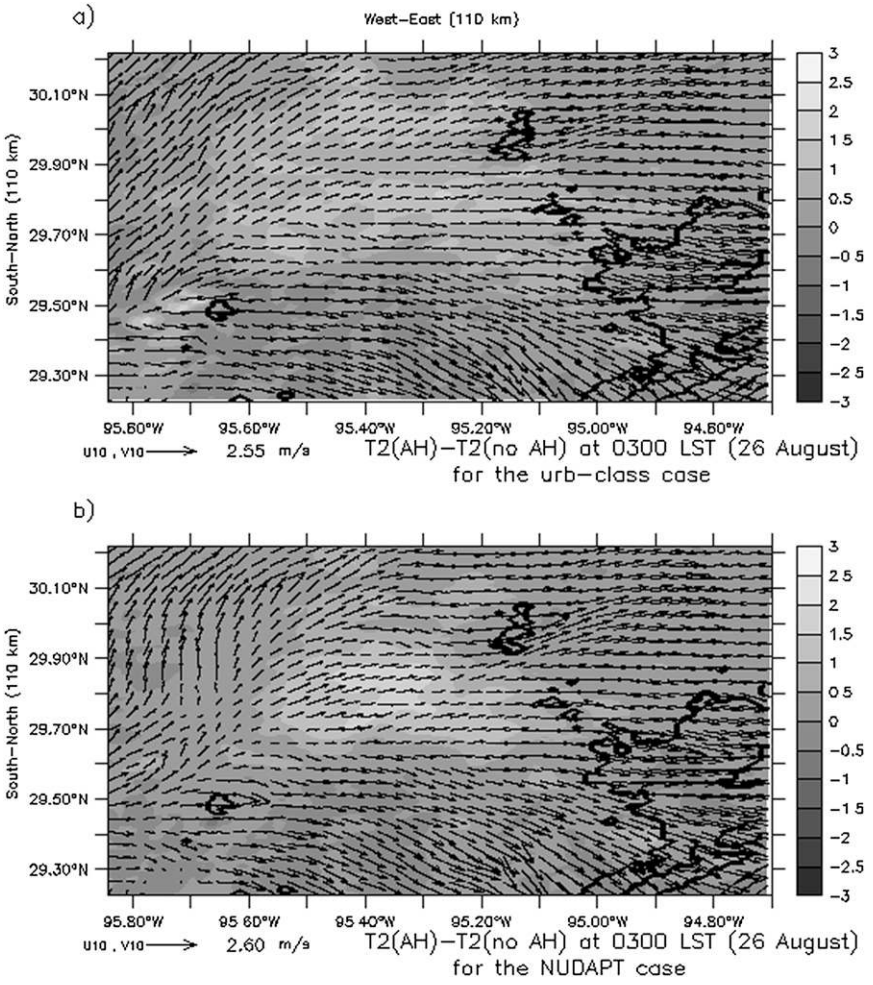

FIG. 14. (a) The 2-m air temperature differences [T2(AH) − T2(no AH)] at 0300 LST (26 Aug) obtained with the BEP+BEM (urb_class) simulation. The wind speed (AH) at 10 m AGL is shown. (b) As in (a), but for the BEP+BEM (NUDAPT) simulation.

different urban configurations, NUDAPT and urb_class. The patterns of the simulated temperature fields present significant differences, showing the impact of the meteorological conditions and the urban morphology in the quantification and spatial distribution of the AH in a city. It is interesting to observe (see Figs. 14b and 15b) that the UHI strength reflects closely the urban fraction. In agreement with other studies (Ohashi et al. 2007), the waste heat increased the air temperature by 0.5°–2°C depending on the location inside the city and the day considered (meteorological conditions).

5. Conclusions

In this article, four urban canopy schemes coupled to the WRF model have been evaluated over the city of Houston, Texas. The first scheme is a BULK scheme, the second is a single-layer urban model with a fixed diurnal profile for the anthropogenic heat (UCM+AH), the third parameterization is a multilayer urban model (BEP), and the last scheme is a multilayer urban parameterization with a building energy model that estimates the anthropogenic heat due to air conditioning (BEP+BEM). For these simulations, an up-to-date urban land cover dataset was used to define three different urban classes for the built-up areas in the numerical domain. Good results (HR $>$ 0.5 for all the stations) for the 2-m air temperature were obtained with the four schemes for 25 August. However, for 31 August, which was hotter than 25 August, the UCM+AH parameterization was not able to capture satisfactorily the temporal evolution of the surface air temperature during the afternoon and the night (in some stations HR $<$ 0.5). In general the BULK scheme tends to overestimate the air temperature while the other schemes to underestimate it. For the wind, BULK and UCM+AH tend to

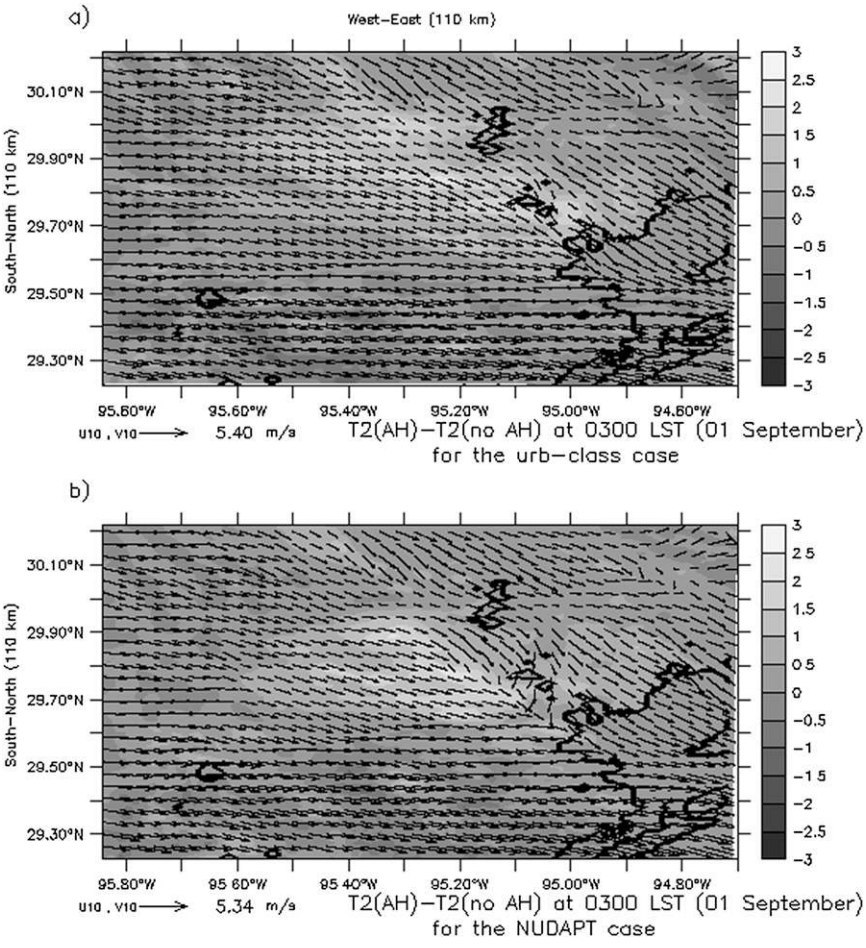

FIG. 15. As in Fig. 14, but for 1 Sep.

overestimate the wind speed whereas BEP and BEP+BEM underestimate it.

To evaluate whether the results can be improved by using a detailed high-resolution gridded UCP database called NUDAPT (instead of urban classes derived from NLCD), new simulations (using this detailed information to define the morphological parameters) were performed with the BEP and BEP+BEM schemes. Results show that the use of detailed information on urban morphology improves the 2-m air temperatures forecast in the majority of stations. However, results obtained with the BEP scheme are less sensitive to the urban morphology than those obtained with the BEP+BEM scheme. The reason is that the AH (computed only in BEP+BEM) is strongly dependent on the urban geometry of the city. To evaluate the impact of AH on air temperature a simulation with BEP+BEM was performed without ejecting the air conditioning into the atmosphere. Results show that AH increased the air temperature up to 2°C during the night in some region of the city.

Finally, the energy consumption due to air conditioning over Houston was quantified with the BEP+BEM scheme for the two days simulated. Differences up to 20% in the EC were obtained due to the different meteorological conditions existing between the two selected days. Moreover, when the NUDAPT data are used, the EC obtained is within a factor of 1.7–2.2 of the monthly data of energy consumption obtained with completely different approaches (bottom-up and top-down). This is a reasonable value taking into account the limitations and uncertainties of an urban canopy parameterization.

In view of these results, if the purpose of the simulation is to quantify the AH, the use of a high-resolution UCP database is a significant help. To study the impact of the AH on the air temperature and evaluate strategies for the mitigation of the UHI and reduction of the EC, an urban scheme like the one (BEP+BEM) presented here is necessary. On the other hand, if the purpose of the simulation is different, for example real-time weather prediction, the BULK scheme produces good estimations

of the meteorological variables, and high-resolution UCP are not necessary.

Indeed, these are the first conclusions that can be derived for this specific case based mainly on 2-m temperature. To reach more complete conclusions more detailed studies must be carried out over different cities and for longer period, examining the whole structure of the PBL, cloud formation, air pollution dispersion, and so on.

Acknowledgments. We thank CIEMAT for the doctoral fellowships held by Francisco Salamanca. We also thank Jason Ching for providing the urban canopy parameters for the city of Houston, Michael Duda for his help in the implementation of the high-resolution urban dataset in the preprocessor of WRF, and Angelines Alberto Morillas for her help in the setup of the computer cluster of CIEMAT where some simulations were performed. Last, we thank Cody Phillips for editing the manuscript. This work was funded by the Ministry of Environment of Spain.

REFERENCES

Bougeault, P., and P. Lacarrère, 1989: Parameterization of orography-induced turbulence in a mesobeta-scale model. *Mon. Wea. Rev.,* **117,** 1872–1890.

Burian, S. J., and W. S. Han, 2003: Morphological analyses using 3D building databases: Houston, Texas. Los Alamos National Laboratory Rep. LA-UR-03-8633, 67 pp.

——, ——, S. P. Velugubantla, and S. R. K. Maddula, 2003: Development of gridded fields of urban canopy parameters for models–3/CMAQ/MM5. EPA Internal Rep. for Contract PO-2D-6217-NTEX, 89 pp.

Chen, F., and J. Dudhia, 2001: Coupling an advanced land surface–hydrology model with the Penn State–NCAR MM5 modeling system. Part I: Model implementation and sensitivity. *Mon. Wea. Rev.,* **129,** 569–585.

——, and Coauthors, 2011: The integrated WRF/urban modelling system: Development, evaluation, and applications to urban environmental problems. *Int. J. Climatol.,* **31,** 273–288, doi:10.1002/joc.2158.

Ching, J., and Coauthors, 2009: National Urban Database and Access Portal Tool. *Bull. Amer. Meteor. Soc.,* **90,** 1157–1168.

DOE, 2005: EnergyPlus Engineering Reference: The Reference to EnergyPlus Calculations. U.S. Department of Energy. [Available online at http://apps1.eere.energy.gov/buildings/energyplus/energyplus_documentation.cfm.]

Dudhia, J., 1989: Numerical study of convection observed during the Winter Monsoon Experiment using a mesoscale two-dimensional model. *J. Atmos. Sci.,* **46,** 3077–3107.

Ek, M. B., K. E. Mitchell, Y. Lin, E. Rogers, P. Grunmann, V. Koren, G. Gayno, and J. D. Tarpley, 2003: Implementation of Noah land surface model advances in the National Centers for Environmental Prediction operational mesoscale Eta model. *J. Geophys. Res.,* **108,** 8851, doi:10.1029/2002JD003296.

Grimmond, C. S. B., and Coauthors, 2010: The International Urban Energy Balance Models Comparison Project: First results from phase 1. *J. Appl. Meteor. Climatol.,* **49,** 1268–1292.

Heiple, S., and D. J. Sailor, 2008: Using building energy simulation and geospatial modeling techniques to determine high resolution building sector energy consumption profiles. *Energy Build.,* **40,** 1426–1436.

Hong, S.-Y., J. Dudhia, and S.-H. Chen, 2004: A revised approach to ice microphysical processes for the bulk parameterization of clouds and precipitation. *Mon. Wea. Rev.,* **132,** 103–120.

Janjic, Z. I., 1994: The step-mountain eta coordinate model: Further developments of the convection, viscous sublayer, and turbulence closure schemes. *Mon. Wea. Rev.,* **122,** 927–945.

Kanda, M., T. Kawai, M. Kanega, R. Moriwaki, K. Narita, and A. Hagishima, 2005: A simple energy balance model for regular building arrays. *Bound.-Layer Meteor.,* **116,** 423–443.

Kikegawa, Y., Y. Genchi, H. Yoshikado, and H. Kondo, 2003: Development of a numerical simulation system toward comprehensive assessments of urban warming countermeasures including their impacts upon the urban buildings' energy demands. *Appl. Energy,* **76,** 449–466.

Kondo, H., Y. Genchi, Y. Kikegawa, Y. Ohashi, H. Yoshikado, and H. Komiyama, 2005: Development of a multilayer urban canopy model for the analysis of energy consumption in a big city: Structure of the urban canopy model and its basic performance. *Bound.-Layer Meteor.,* **116,** 395–421.

Kusaka, H., and F. Kimura, 2004: Coupling a single-layer urban canopy model with a simple atmospheric model: Impact on urban heat island simulation for an idealized case. *J. Meteor. Soc. Japan,* **82,** 67–80.

——, H. Kondo, Y. Kikegawa, and F. Kimura, 2001: A simple single-layer urban canopy model for atmospheric models: Comparison with multi-layer and slab models. *Bound.-Layer Meteor.,* **101,** 329–358.

Lin, C.-Y., F. Chen, J. C. Huang, W.-C. Chen, Y.-A. Liou, W.-N. Chen, and S.-C. Liu, 2008: Urban heat island effect and its impact on boundary layer development and land–sea circulation over northern Taiwan. *Atmos. Environ.,* **42,** 5635–5649.

Liu, Y., F. Chen, T. Warner, and J. Basara, 2006: Verification of a mesoscale data-assimilation and forecasting system for the Oklahoma City area during the Joint Urban 2003 Field Project. *J. Appl. Meteor. Climatol.,* **45,** 912–929.

Lo, J. C. F., A. K. H. Lau, F. Chen, J. C. H. Fung, and K. K. M. Leung, 2007: Urban modification in a mesoscale model and the effects on the local circulation in the Pearl River Delta region. *J. Appl. Meteor. Climatol.,* **46,** 457–476.

Martilli, A., A. Clappier, and M. W. Rotach, 2002: An urban surface exchange parameterisation for mesoscale models. *Bound.-Layer Meteor.,* **104,** 261–304.

——, Y.-A. Roulet, M. Junier, F. Kirchner, M. W. Rotach, and A. Clappier, 2003: On the impact of urban surface exchange parameterisations on air quality simulations: The Athens case. *Atmos. Environ.,* **37,** 4217–4231.

Masson, V., 2000: A physically-based scheme for the urban energy budget in atmospheric models. *Bound.-Layer Meteor.,* **94,** 357–397.

Miao, S., F. Chen, M. A. LeMone, M. Tewari, Q. Li, and Y. Wang, 2009: An observational and modeling study of characteristics of urban heat island and boundary layer structures in Beijing. *J. Appl. Meteor. Climatol.,* **48,** 484–501.

Mlawer, E. J., S. J. Taubman, P. D. Brown, M. J. Iacono, and S. A. Clough, 1997: Radiative transfer for inhomogeneous atmospheres: RRTM, a validated correlated-*k* model for the longwave. *J. Geophys. Res.,* **102** (D14), 16 663–16 682.

Ohashi, Y., Y. Genchi, H. Kondo, Y. Kikegawa, H. Yoshikado, and Y. Hirano, 2007: Influence of air-conditioning waste heat on

air temperature in Tokyo during summer: Numerical experiments using an urban canopy model coupled with a building energy model. *J. Appl. Meteor. Climatol.,* **46,** 66–81.

Salamanca, F., and A. Martilli, 2010: A new building energy model coupled with an urban canopy parameterization for urban climate simulations—Part II. Validation with one dimension off-line simulations. *Theor. Appl. Climatol.,* **99,** 345–356.

——, A. Krpo, A. Martilli, and A. Clappier, 2010: A new building energy model coupled with an urban canopy parameterization for urban climate simulations—Part I. Formulation, verification and a sensitive analysis of the model. *Theor. Appl. Climatol.,* **99,** 331–344.

Sertel, E., A. Robock, and C. Ormeci, 2010: Impacts of land cover data quality on regional climate simulations. *Int. J. Climatol.,* **30,** 1942–1953, doi:10.1002/joc.2036.

Skamarock, W. C., and Coauthors, 2008: A description of the Advanced Research WRF version 3. NCAR Tech. Note TN-475+STR, 125 pp.